Langerhans cells are generated by two distinct PU.1-dependent transcriptional networks

Michaël Chopin,[1,2] Cyril Seillet,[1,2] Stéphane Chevrier,[1,2] Li Wu,[1,2,3] Hongsheng Wang,[4] Herbert C. Morse III,[4] Gabrielle T. Belz,[1,2] and Stephen L. Nutt[1,2]

[1]The Walter and Eliza Hall Institute of Medical Research, Parkville, Victoria 3052, Australia
[2]Department of Medical Biology, University of Melbourne, Parkville, Victoria 3010, Australia
[3]Tsinghua-Peking University Joint Centre for Life Sciences, Tsinghua University School of Medicine, Beijing 100084, China
[4]Laboratory of Immunogenetics, National Institute of Allergy and Infectious Diseases, National Institutes of Health, Rockville, MD 20852

Langerhans cells (LCs) are the unique dendritic cells found in the epidermis. While a great deal of attention has focused on defining the developmental origins of LCs, reports addressing the transcriptional network ruling their differentiation remain sparse. We addressed the function of a group of key DC transcription factors—PU.1, ID2, IRF4, and IRF8—in the establishment of the LC network. We show that although steady-state LC homeostasis depends on PU.1 and ID2, the latter is dispensable for bone marrow–derived LCs. PU.1 controls LC differentiation by regulating the expression of the critical TGF-β responsive transcription factor RUNX3. PU.1 directly binds to the *Runx3* regulatory elements in a TGF-β–dependent manner, whereas ectopic expression of RUNX3 rescued LC differentiation in the absence of PU.1 and promoted LC differentiation from PU.1-sufficient progenitors. These findings highlight the dual molecular network underlying LC differentiation, and show the central role of PU.1 in these processes.

CORRESPONDENCE
Stephen Nutt:
nutt@wehi.edu.au

Abbreviations used: cDC, conventional DC; IRES, internal ribosome entry site; LC, Langerhans cell; MCSFR, macrophage colony stimulation factor 1 receptor; MFI, mean fluorescence intensity; pDC, plasmacytoid DC.

DCs are a highly diverse family of related cell types that are distributed throughout the body. They provide a first line of defense against foreign pathogens, while also acting to maintain tolerance to self. DCs can be divided into four major classes. Conventional DCs (cDCs) and plasmacytoid DCs (pDCs) predominate at steady-state, whereas monocyte-derived DCs are the main population in an inflammatory setting (Belz and Nutt, 2012). Langerhans cells (LCs) constitute the fourth major category of DCs. LCs are found in the epidermis and are at the forefront of environmental insults resulting from the breakage of the skin barrier by commensal organisms or environmental antigens.

LCs are distinct from other DC populations not only due to their location but also their differentiation requirements. For instance, pDC and cDC development is intricately linked to their responsiveness to the cytokine Flt3L (Fms-related tyrosine kinase 3 ligand) and its receptor Flt3 (McKenna et al., 2000; Tussiwand et al., 2005; Waskow et al., 2008), as the absence of either factor leads to reduced numbers of cDC and pDC, whereas LC differentiation and frequency are not affected (Onai et al., 2007a; Merad et al., 2008; Waskow et al., 2008). In contrast, LCs are selectively absent in mice lacking either the macrophage colony stimulation factor 1 receptor (MCSFR, also known as CSF1R; Ginhoux et al., 2006) or TGF-β (Borkowski et al., 1996). The finding that LCs are generated in mice carrying a mutation resulting in the inactivation of the gene encoding MCSF (*Csf1*) gene was initially puzzling (Witmer-Pack et al., 1993), but recent studies reconciled this discrepancy by showing that LCs fail to develop in mice lacking IL-34, a stroma-derived cytokine binding with high affinity to the MCSFR (Greter et al., 2012; Wang et al., 2012).

Another striking difference between cDCs and LCs lies in their homeostasis. Although cDCs and pDCs are constantly renewed from $Flt3^+$ BM precursors (Naik et al., 2007; Onai et al., 2007b), steady-state LCs derive from myeloid

The Rockefeller University Press $30.00
J. Exp. Med. 2013 Vol. 210 No. 13 2967-2980
www.jem.org/cgi/doi/10.1084/jem.20130930

precursors that seed the prospective skin very early in embryogenesis (Hoeffel et al., 2012). This epidermal LC progenitor proliferates rapidly during the first few days after birth and subsequently acquires LC-like features such as dendrites and expression of the LC markers CD11c, MHCII, and Langerin (CD207; Tripp et al., 2004; Chorro et al., 2009).

Despite the detailed understanding of the phenotype and function of LCs, our understanding of the transcriptional network driving their differentiation is relatively poor. Studies addressing the signaling mediators downstream of TGF-β signaling highlighted the critical roles for ID2 (Hacker et al., 2003) and RUNX3 in driving LC homeostasis and or differentiation (Fainaru et al., 2004). In addition, a role for the IRF8 (IFN regulator factor 8, also known as ICSBP [IFN consensus sequence binding protein]) in the development and migration of LCs has been proposed, as *Irf8*$^{-/-}$ mice display a twofold reduction in LC frequency in the epidermis and impaired LC trafficking to lymphoid organs (Schiavoni et al., 2004). Another likely candidate regulator of LCs is the ETS family member transcription factor PU.1 (encoded by the *Sfpi1* gene). PU.1 is an essential regulator of many aspects of early hematopoiesis and myeloid cell differentiation (Dakic et al., 2007). Recently, PU.1 was shown to be a crucial transcription factor in controlling *Flt3* expression in a dose-dependent manner, thereby promoting cDC and pDC differentiation (Carotta et al., 2010). A potential role for PU.1 in promoting LC differentiation has been postulated but has not yet been formally shown experimentally, and the molecular basis for such a function remains unexplored (Iwama et al., 2002; Heinz et al., 2006).

In this study, we have examined the requirement of key transcriptional regulators in promoting the differentiation and homeostasis of both steady-state and inflammation-induced LC populations. The removal of PU.1 and ID2 in a DC-specific manner has revealed a central requirement for PU.1 in both types of LCs, whereas ID2 was essential for steady-state, but not inflammation-derived LCs. We show that PU.1 regulates the expression of the essential LC gene *Runx3* in a TGF-β–dependent manner, a finding which highlights how a broadly expressed transcription factor such as PU.1 can have a context-specific role in LCs. Thus, the dual origin of the LC network relies on two distinct transcriptional networks, both of which are governed by PU.1.

RESULTS

Transcription factor expression in LCs

To better define the transcriptional network controlling LC differentiation, the expression of the transcription factors PU.1, ID2, IRF4, and IRF8 was analyzed by flow cytometry. PU.1 and ID2 expression was monitored using our reporter strains where an IRES (internal ribosome entry site)-eGFP cassette has been inserted into the 3′ untranslated region of the *Sfpi1* and *Id2* genes, generating PU.1^{GFP} and ID2^{GFP} reporters, respectively (Nutt et al., 2005; Jackson et al., 2011). PU.1 and ID2 were both constitutively expressed in epidermal LCs, and the expression of the latter increased on migration to the skin draining LNs (Fig. 1 A).

Homozygous knockin mice harboring eGFP fused to the C terminus of the IRF8 protein were used to follow IRF8^{GFP} expression (unpublished data). IRF8 was relatively lowly expressed in epidermal LC but strongly up-regulated in the migratory LCs in LNs (Fig. 1 A). Similarly, intracellular staining for IRF4 revealed that LCs did not express IRF4 in the epidermis; however, IRF4 expression was up-regulated in the LN LCs (Fig. 1 A).

PU.1 and ID2, but not IRF4 and IRF8, are required for the generation of LC

To rigorously assess the function of PU.1, ID2, IRF4, and IRF8 in LC differentiation, mice harboring floxed alleles of each gene were crossed to *Itgax*^{cre} mouse, whereby Cre-mediated deletion is under the control of the CD11c promoter (Caton et al., 2007). This led to the generation of four new mouse strains: *Itgax*^{cre}*Sfpi1*$^{fl/fl}$, *Itgax*^{cre}*Irf4*$^{fl/fl}$, *Itgax*^{cre}*Irf8*$^{fl/fl}$, and *Itgax*^{cre}*Id2*$^{fl/fl}$, hereafter named PU.1cKO, IRF4cKO, IRF8cKO, and Id2cKO, respectively.

The presence of LCs in the epidermis of each of the mouse strains was followed by flow cytometry. This showed an almost complete loss of epidermal CD11c^{+}MHCII^{+} LCs in PU.1cKO and Id2cKO mice (Fig. 1 B). LC loss was also apparent after immunohistochemical staining for Langerin in epidermal sheets from adult mouse (Fig. 1 C). Deletion of either IRF4 or IRF8 in CD11c-expressing cells had no effect on the frequency of LCs found in the epidermis, a finding consistent with our observation that these transcription factors were very lowly expressed in epidermal LCs (Fig. 1, A and B). To further corroborate these findings, LC cells were enumerated from epidermal sheets of *Irf4*$^{-/-}$ and *Irf8*$^{-/-}$ mice. Consistently with our observations using cKO mice, neither factor was required for the generation of normal numbers of LCs (unpublished data). Although our finding contrasts with a previous study using *Irf8*$^{-/-}$ mice that found a twofold reduction in the frequency of LCs (Schiavoni et al., 2004), our results are consistent with the recent findings on human harboring mutations in IRF8 disrupting its interaction with the DNA (Hambleton et al., 2011) and unpublished observation in the mouse that LC generation is largely independent of IRF8 (Hashimoto et al., 2011).

As expected, the frequency of migratory DCs was severely reduced in the peripheral LNs of PU.1cKO and Id2cKO mice (Fig. 1 D). In the case of PU.1, while all migratory DCs were reduced in number, the majority of the remaining Langerin^{+} cells found in the skin-draining LN coexpressed CD103, which marks a subset of migrating dermal DCs (Bursch et al., 2007; Fig. 1 E–G). In keeping with previous findings, both the CD103^{+}Langerin^{+} dermal DCs and CD103^{-}Langerin^{+} LC compartments were severely reduced in the absence of ID2 (Hacker et al., 2003; Ginhoux et al., 2009; Fig. 1, E–G).

Ablation of IRF8 did not strongly impair the egress of LCs from the skin, as the frequency of migratory LCs found in the LN mirrored the wild-type controls (Fig. 1 D). Importantly,

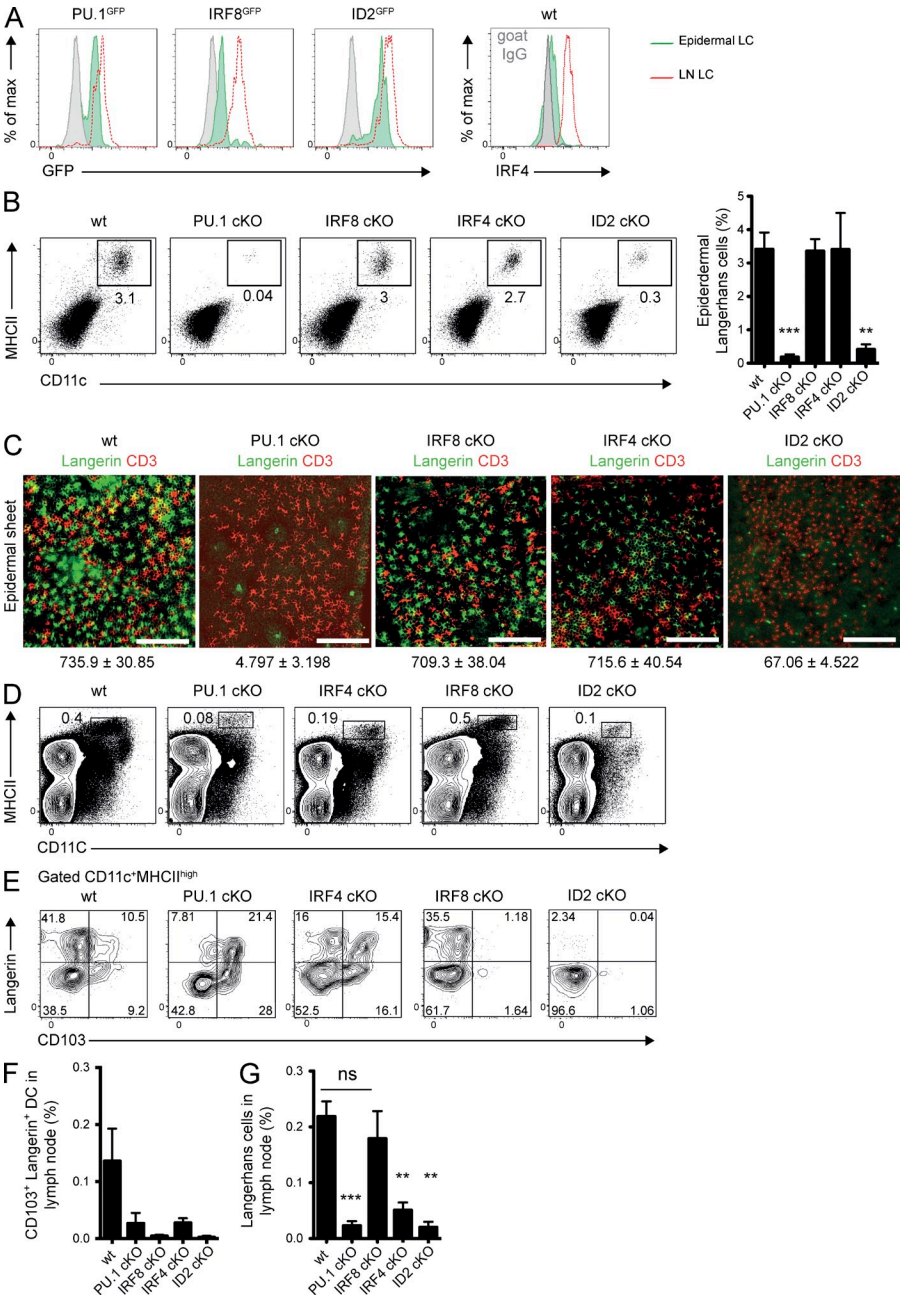

Figure 1. PU.1 and ID2 are essential for the steady-state differentiation of LCs. (A) Left, reporter mice of the indicated genotypes were assessed for the expression of GFP in epidermis (green) and migratory LN (red). Gray histograms show autofluorescence in LCs isolated from wild-type (wt) epidermis. Right, IRF4 expression was analyzed intracellular by flow cytometry from the same populations from a wild-type mouse. Gray histogram shows the background staining from a goat IgG isotype control. Results are representative of three experiments. (B) Epidermal sheets from mice of the indicated genotype were analyzed for CD11c and MHCII expression. Numbers represent the frequency of CD11c$^+$MHCII$^+$ LCs in the epidermis of a representative mouse of each genotype. Graph shows the mean proportion of epidermal CD11c$^+$MHCII$^+$ LCs ± SD from at least six mice per genotype. **, $P < 0.01$; ***, $P < 0.001$ (unpaired Student's *t* test) compared with wild-type sample. (C) Epidermal sheets from mice of the indicated genotype stained for CD3ε (red, indicative of T cells) and Langerin (green, LCs) and analyzed by immunofluorescence microscopy. Bars, 80 µM. Data are representative of three experiments. Numbers below represent the mean density of LCs/mm^2 ± SD from 20 fields per genotype. (D) Flow cytometric of CD11c and MHCII expression in peripheral LN of the indicated genotype. Number represents the frequency of CD11c$^+$MHCII^{high} migratory DCs. Results are representative of six mice. (E) Flow cytometry of Langerin and CD103 expression in CD11c$^+$MHCII^{high} gated cells (as in D) from the peripheral LN cells of the indicated genotype. Numbers represent the frequency of cells within the indicated quadrant. Data are representative of three independent experiments. (F and G) Bar graphs show the mean proportion ± SD of CD103$^+$langerin$^+$ DCs (F) and CD103$^-$langerin$^+$ LCs (G), gated as in E, from at least six mice per genotype. **, $P < 0.01$; ***, $P < 0.001$ (unpaired Student's *t* test) compared with wild-type sample. ns, not significant, $P > 0.05$.

migratory CD103$^+$ dermal DCs were absent from the LNs of IRF8cKO, consistent with previous studies and confirming that CD11c-driven deletion was efficient at this locus (Fig. 1 E). In keeping with the up-regulation in IRF4 expression upon migration, the frequency of migratory LCs in peripheral LNs was greatly reduced in IRF4cKO (Fig. 1, D–G). Collectively, these data highlight the pivotal and DC-intrinsic role of PU.1 and ID2 for the development and or maintenance of epidermal LC.

In vitro generated LCs

To systematically investigate the role of different transcription factors during LC differentiation, an in vitro system that supports LC development was needed. TGF-β1 is critical for LC differentiation in vivo (Borkowski et al., 1996, 1997; Becker et al., 2011) and has been shown to cooperate with GM-CSF to drive the differentiation of CD14$^+$ human monocytes into LCs (Geissmann et al., 1998). Consistently, Becker et al. (2011) have recently described an in vitro system, where the addition of TGF-β to BM precursors cultured in the presence of MCSF and GM-CSF could readily generate LC-like cells. To examine this differentiation system in more detail, BM cells were cultured with GM-CSF and TGF-β for 3 d. Examination of the CD11c$^+$MHCII$^+$ component of the resulting cultures showed the presence of four phenotypically

distinct populations based on the expression of DEC205 and EPCAM, markers commonly used to delineate LCs (Fig. 2 A). While all four fractions arose from a TGF-β responsive precursor, which had undergone multiple cell divisions, their relative abundance was dependent on the TGF-β concentration (Fig. S1, A–C). Furthermore, GM-CSF was also found to be essential in this culture system, as DEC205$^+$EPCAM$^+$ DCs could not be generated from BM precursors cultivated in the presence of MCSF alone or supplemented with TGF-β (Fig. S1 D).

To better understand the relationship between these different populations induced by GM-CSF and TGF-β, the four fractions were sorted by flow cytometry and recultured for a further 24 h before reanalysis (Fig. 2 B). Fraction I, defined as DEC205$^-$EPCAM$^-$ retained multipotent potential as these cells generated all four subsets. Fraction II (DEC205$^+$EPCAM$^-$) failed to generate any other population and is likely to be terminally differentiated. Fraction III (DEC205$^-$EPCAM$^+$), differentiated predominantly into the DEC205$^+$EPCAM$^+$ fraction IV, while fraction IV cells maintained their identity but showed a further up-regulation of DEC205 (Fig. 2 B).

To characterize the lineage identity of these four different fractions, cells were sorted according to EPCAM and DEC205 cell surface expression. Cytospins of each population were stained with hematoxylin and eosin and analyzed for cellular morphology. Consistent with the above finding that fraction I maintained some developmental plasticity, this fraction retained a variety of cells in size and shape, while fraction II was highly enriched for cells with macrophage morphology. Fractions III and IV were more homogeneously small in size and presented small cytoplasmic protrusions (Fig. 2 C). Although Langerin expression is known to be relatively low in this culture system (Becker et al., 2011), we found that the mRNA for *Cd207* (encoding Langerin) was exclusively found in

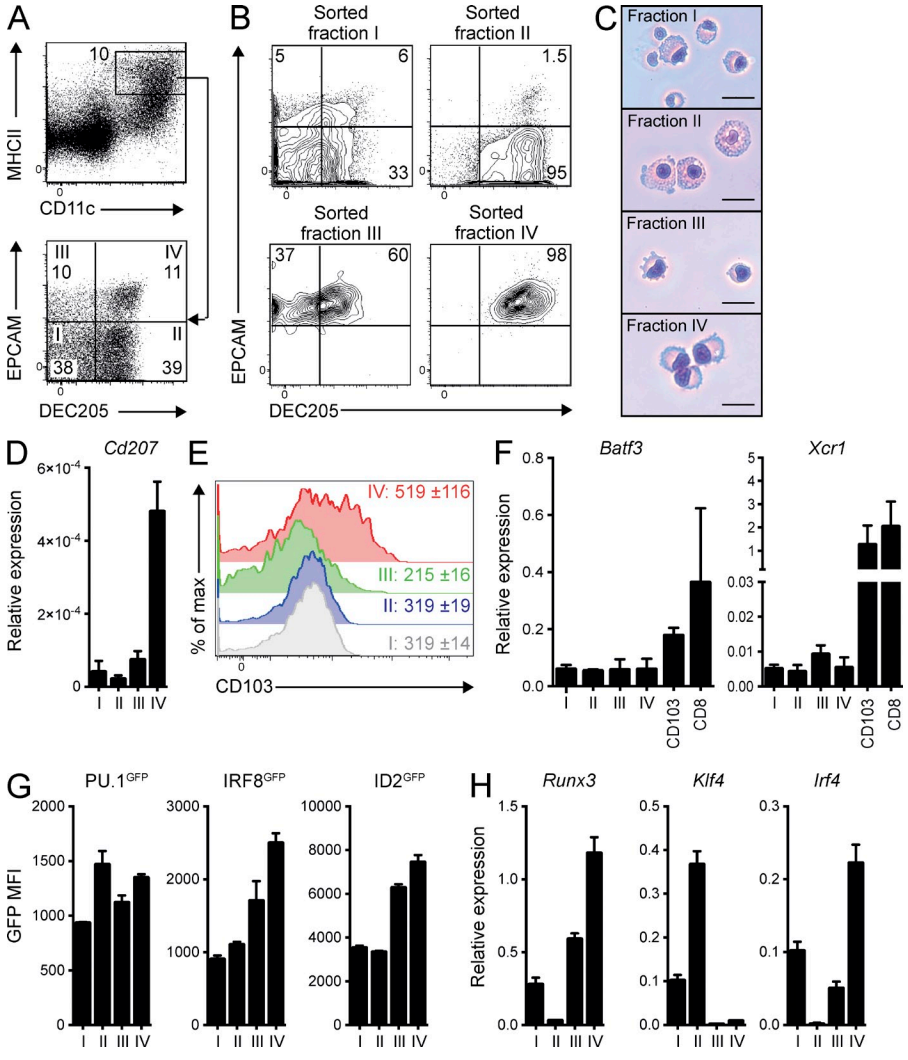

Figure 2. In vitro generated LCs. (A) Wild-type (wt) BM cells were cultured for 3 d in the presence of GM-CSF and TGF-β. Dot plots represent the expression of DEC205 and EPCAM within the CD11c$^+$MHCII$^+$ compartment. Data are representative of three independent experiments. (B) Fractions I to IV as depicted in A were sorted and recultured for 24 h in the presence of GM-CSF and TGF-β. Plots show the expression of DEC205 and EPCAM for the indicated fraction and the proportion of cells in each quadrant. (C) Indicated fractions identified as in A were sorted by flow cytometry and morphology was assessed by microscopy. Data in B and C are representative of two independent experiments. Bars, 10 µM. (D) Quantitative real-time PCR for the expression of *Cd207* in fractions I to IV sorted as in A. Values are normalized to *Hprt* and are the mean ± SD from three experiments. (E) Histograms represent CD103 expression on the indicated fractions identified as in A. Numbers represent the geometric mean fluorescence intensity (MFI) ± SD from three experiments. (F) Quantitative real-time PCR for the expression of *Xcr1* and *Batf3* in fractions I to IV sorted as in A. In vitro generated CD103$^+$ DCs, and ex vivo isolated splenic CD8$^+$ DCs were positive controls. Values are normalized to *Hprt* and are the mean ± SD from two experiments. (G) BM cells from reporter mice of the indicated genotype were cultured for 3 d in the presence of GM-CSF and TGF-β and expression of GFP was analyzed within the different gated fractions. Bar graphs show the MFI ± SD of the gated fractions from three mice per genotype. Data are representative of two independent experiments. (H) Quantitative real-time PCR for the expression of key transcription factors in fractions I to IV sorted as in A. Values are normalized to *Hprt* and are the mean ± SD from three experiments.

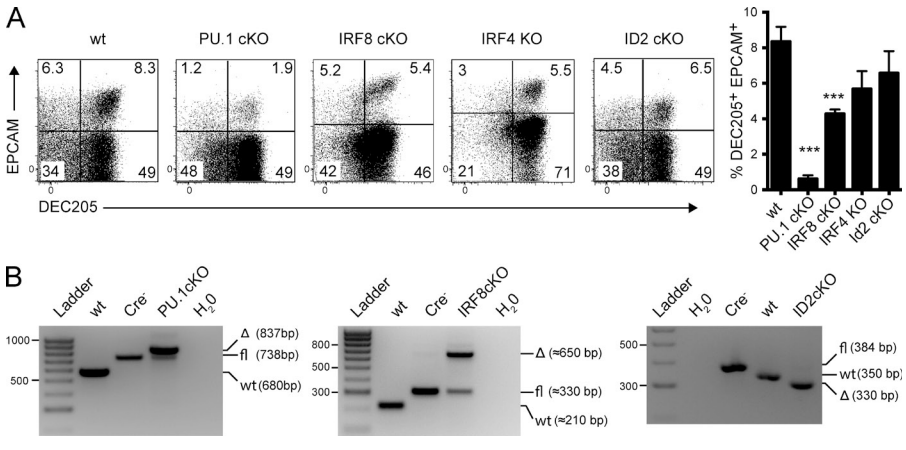

Figure 3. In vitro generated LCs require PU.1 but not ID2. (A) BM cells from the indicated genotype were cultured in the presence of GM-CSF and TGF-β. At day 3, CD11c$^+$MHCII$^+$ cells were monitored by flow cytometry for their expression of DEC205 and EPCAM. A representative plot for each genotype is shown. Numbers represent the frequency of CD11c$^+$MHCII$^+$ cells generated for the indicated genotype. Bar graphs show the mean proportion ± SD of in vitro generated LC from at least four experiments per genotype. ***, $P < 0.001$ (unpaired Student's *t* test) compared with the wild-type sample. Data from IRF4-deficient (IRF4 KO) cells are from *Irf4*$^{-/-}$ mice. (B) BM cells from the indicated genotype were cultured in the presence of GM-CSF and TGF-β. At day 3, CD11c$^+$MHCII$^+$ cells were sorted and DNA extracted. The deletion efficiency was assessed by PCR. Cre$^-$, cells derived from the respective *fl/fl Itgax*$^{cre+/+}$ mice; H_2O, no DNA added to the reaction. The position of the wild-type (wt), loxP flanked (fl), and deleted (Δ) alleles are shown for each genotype. Data are representative of three independent experiments.

Fraction IV, suggesting that this fraction contained cells with a more mature phenotype than those found in fraction III (Fig. 2 D). To further define the nature of these in vitro generated LC-like cells, CD103 expression was measured by flow cytometry. CD103 is a marker commonly used to distinguish LCs (Langerin$^+$CD103$^-$) from CD103$^+$ DCs (Langerin$^+$CD103$^+$), although GM-CSF is known to induce CD103 expression in non-CD103$^+$ DC subsets in vitro (Edelson et al., 2011; Jackson et al., 2011; Sathe et al., 2011). Despite CD103 expression being higher in fraction IV (Fig. 2 E), these cells lacked the transcriptional signature of CD103$^+$ DCs, as the expression of the key transcription factor BATF3, and the chemokine receptor XCR1 was much lower than in conventional CD103$^+$ and CD8$^+$ DCs (Fig. 2 E; Hildner et al., 2008; Edelson et al., 2010; Crozat et al., 2011; Bachem et al., 2012). In keeping with their expression in LCs in vivo, the mean fluorescence index of ID2^{GFP} and IRF8^{GFP} increased in fractions III and IV, whereas PU.1 expression was uniform in all populations (Fig. 2 G).

In DCs, the TGF-β–induced response is mediated by the transcription factor RUNX3 (Fainaru et al., 2004). Although all cells were exposed to TGF-β, qPCR analysis revealed that *Runx3* expression was restricted to fractions III and IV, confirming that these cells arose from a TGF-β responsive BM precursor (Fig. 2 H). In contrast, *Klf4* (*Krüppel-like factor 4*), a transcription factor essential for macrophage function (Liao et al., 2011), was highly enriched in fraction II, whereas Irf4 showed a reciprocal expression pattern. (Fig. 2 H). Collectively, these observations highlight the fact that TGF-β–driven DEC205$^+$EPCAM$^+$ cells express a transcriptional profile and morphological features consistent with those of LCs.

In vitro generated LCs require PU.1 but not ID2

We next examined whether in vitro BM-derived LCs rely on the same transcriptional machinery as LCs generated in vivo by culturing BM cells from cKO mice cultured in the presence of GM-CSF and TGF-β. 3 d after stimulation, cells were harvested and stained for their surface expression of CD11c, MHCII, DEC205, and EPCAM. Generation of LCs in vitro was observed from IRF4cKO (not depicted), *Irf4*$^{-/-}$ (IRF4 KO), and IRF8cKO BM, albeit for the latter to a lesser extent than from wild-type BM (Fig. 3 A). In contrast, PU.1 was required for the formation of DEC205$^+$EPCAM$^+$ BM-derived LCs. Surprisingly deletion of ID2 in CD11c-expressing cells did not impair the in vitro generation of BM-derived LCs (Fig. 3 A), in striking contrast to the loss seen in vivo (Fig. 1, B and D). Using a PCR-based assay, we confirmed the efficient Cre-mediated excision of the targeted PU.1, IRF8, and ID2 cKO alleles occurred in the CD11c$^+$MHCII$^+$ cells generated in these cultures (Fig. 3 B). These observations suggest that the in vitro BM-derived LCs represent a distinct subset that is dependent on PU.1 expression but independent of ID2.

PU.1 is required for LC repopulation of the skin under inflammatory conditions

Experimental evidence has pointed to a potential dual origin of the LC network. After UV exposure, epidermal LCs are severely reduced. The resulting inflammation leads to the recruitment of blood-borne monocytes to the injured skin where they differentiate into LCs (Ginhoux et al., 2006). Although replenishment of the LC network is dependent on MCSFR-driven signaling, differentiation is independent of IL34 (Greter et al., 2012; Wang et al., 2012).

Following from this, we propose that as inflammatory and steady-state LCs originate from distinct precursors, the transcriptional machinery guiding their differentiation is likely to be different. Before testing this hypothesis, it was necessary to first ascertain that blood monocytes subsets were not affected by the loss of PU.1 or ID2 in CD11c-expressing cells. Circulating CD11b$^+$MCSFR$^+$ cells can be divided into Ly6C^{low}CD11c$^+$ CX3CR1^{high} resident monocytes and Ly6C^{high}CD11c$^-$ CX3CR1^{low} inflammatory monocytes (Geissmann et al., 2003;

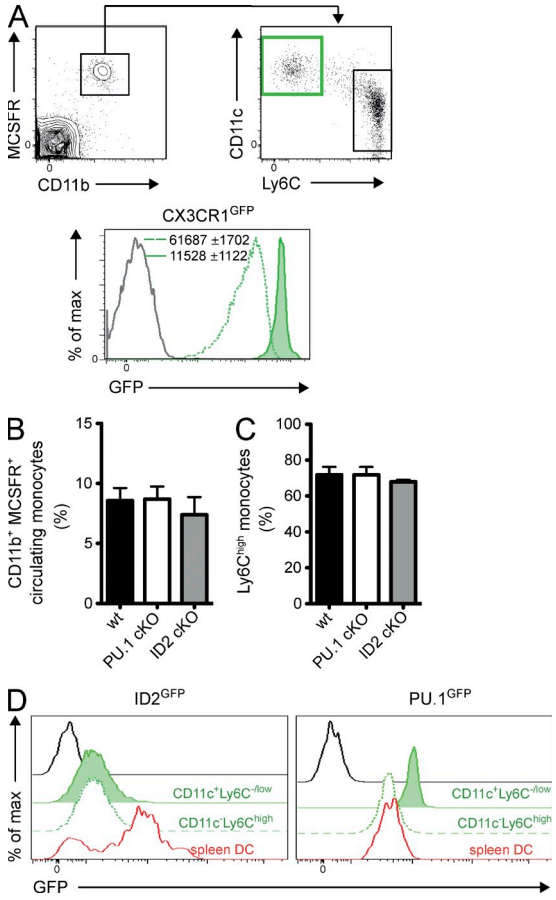

Figure 4. Characterization of the expression of PU.1 and ID2 in circulating monocytes. (A) Circulating mononuclear cells were isolated from blood and analyzed by flow cytometry. CD11b$^+$MCSFR$^+$ monocytes (left plot) were gated and the expression of Ly6C and CD11c was analyzed (right plot). Histograms represent the expression of CX3CR1 using CX3CR1^{GFP} reporter mouse on inflammatory CD11c$^-$ly6C^{high} monocytes (dashed green histogram) and resident CD11c$^+$ly6C$^{-/low}$ monocytes (green filled histogram). (B and C) The mean of frequency of total CD11b$^+$MCSFR$^+$ circulating monocytes (B) and CD11b$^+$MCSFR$^+$ CD11c$^-$Ly6C^{high} inflammatory monocytes (C) are shown. The data are the mean ± SD from five mice. (D) Reporter mice of the indicated genotypes were assessed for the expression of GFP in in the CD11b$^+$MCSFR$^+$CD11c$^-$Ly6C^{high} (dashed green line) and CD11b$^+$MCSFR$^+$ CD11c$^+$Ly6C$^{-/low}$ (filled green line) compartments. Gray histograms show autofluorescence in identical populations isolated from wild type blood. Numbers represents the MFI of GFP for the indicated population ± SD. Data are representative of two independent experiments.

Fig. 4 A), with Itgax^{cre} activity being restricted to resident monocytes (Caton et al., 2007; Gaiser et al., 2012). Both populations were found in normal numbers in PU.1cKO and ID2cKO mice (Fig. 4, B and C), demonstrating that any Cre-mediated gene deletion in monocytes did not impact on their frequency and thus potential to respond to the inflammatory signals that induced LC repopulation. To further characterize those monocytes, expression of PU.1^{GFP} and ID2^{GFP} within those populations was monitored by flow cytometry. Both populations expressed low levels of ID2 compared with splenic DCs, whereas PU.1 expression in inflammatory monocytes was similar to the levels of splenic cDCs, while resident monocytes expressed higher PU.1 (Fig. 4 D).

We then tested whether either PU.1 or ID2 were required for the differentiation of BM-derived LCs after skin injury induced by UV exposure. To this end, lethally irradiated C57BL/6 Ly5.1$^+$ mice were reconstituted with wild-type, PU.1cKO, or ID2cKO BM (all Ly5.2$^+$, Fig. 5 A). 6 wk after reconstitution, mice were exposed to UV light for 30 min to deplete host LCs. 3 wk after UV exposure, the recruitment of donor Ly5.2$^+$ cells into the epidermis was monitored by flow cytometry. As expected, BM-derived Ly5.2$^+$ LCs were generated in Ly5.1$^+$ mice reconstituted with wild-type BM, whereas host Ly5.1$^+$ LCs were severely reduced (Fig. 5 B). Analysis of the ears, trunk epidermis, and LNs of mice reconstituted with Ly5.2$^+$ wild-type, PU.1cKO, or ID2cKO BM revealed a similar the degree of chimerism regardless of donor genotype (Fig. 5 C). Mice reconstituted with Ly5.2$^+$ PU.1cKO BM failed to differentiate into CD11c$^+$MHCII$^+$ epidermal LCs, highlighting the pivotal role of PU.1 in driving their differentiation from a BM-derived precursor (Fig. 5 D). In contrast, LCs were generated in Ly5.1$^+$ mice reconstituted with Ly5.2$^+$ ID2cKO BM (Fig. 5 D). These results perfectly mirrored the results generated using the in vitro LC differentiation system and demonstrate that in contrast to steady-state LC where ID2 is indispensable, inflammatory BM-derived LCs are insensitive to ID2 loss.

Consistent with the above findings, Langerin$^+$ cells in peripheral LNs were severely reduced in mice reconstituted with PU.1cKO, whereas they were only slightly reduced in mice reconstituted with ID2cKO BM (Fig. 5 E). Analysis of the cell surface markers expressed by migratory DCs revealed that the vast majority of Langerin$^+$-expressing cells derived from ID2cKO are CD103$^-$ and therefore represent LCs (Fig. 5 E). In contrast, mice reconstituted with Ly5.2$^+$ PU.1cKO BM contained Langerin$^+$CD103$^+$ dermal DCs and few epidermal LCs (Fig. 5 E).

To determine whether the LCs generated from ID2cKO BM could persist longer-term, we repeated the UV-induced skin injury model described above (Fig. 5 A) and analyzed the LC repopulation 6 wk after UV treatment. ID2cKO-derived LCs (Fig. 5 F), which had efficiently excised the targeted ID2 allele (Fig. 5 G), were still present at the time point, indicative of sustained LC reconstitution.

To gain insights into differential requirement of LCs generated after UV induced skin injury for PU.1 and ID2, we reconstituted lethally irradiated Ly5.1$^+$ mice with either PU.1^{GFP} or Id2^{GFP} BM (both Ly5.2$^+$). 6 wk after reconstitution, mice were exposed to UV, and 3 wk later the epidermis was isolated and analyzed by flow cytometry. Donor-derived cells were able to differentiate into three distinct subsets based on the surface expression of the markers CD11c and MHCII (Fig. 6 A). Both CD11c$^-$MHCII$^-$ and CD11c$^+$MHCII$^-$ cells lacked PU.1^{GFP} and expressed ID2^{GFP} constitutively, whereas the CD11c$^+$MHCII$^+$ LCs expressed high levels of PU.1 and ID2. Thus, despite the induction of ID2 expression in BM-derived

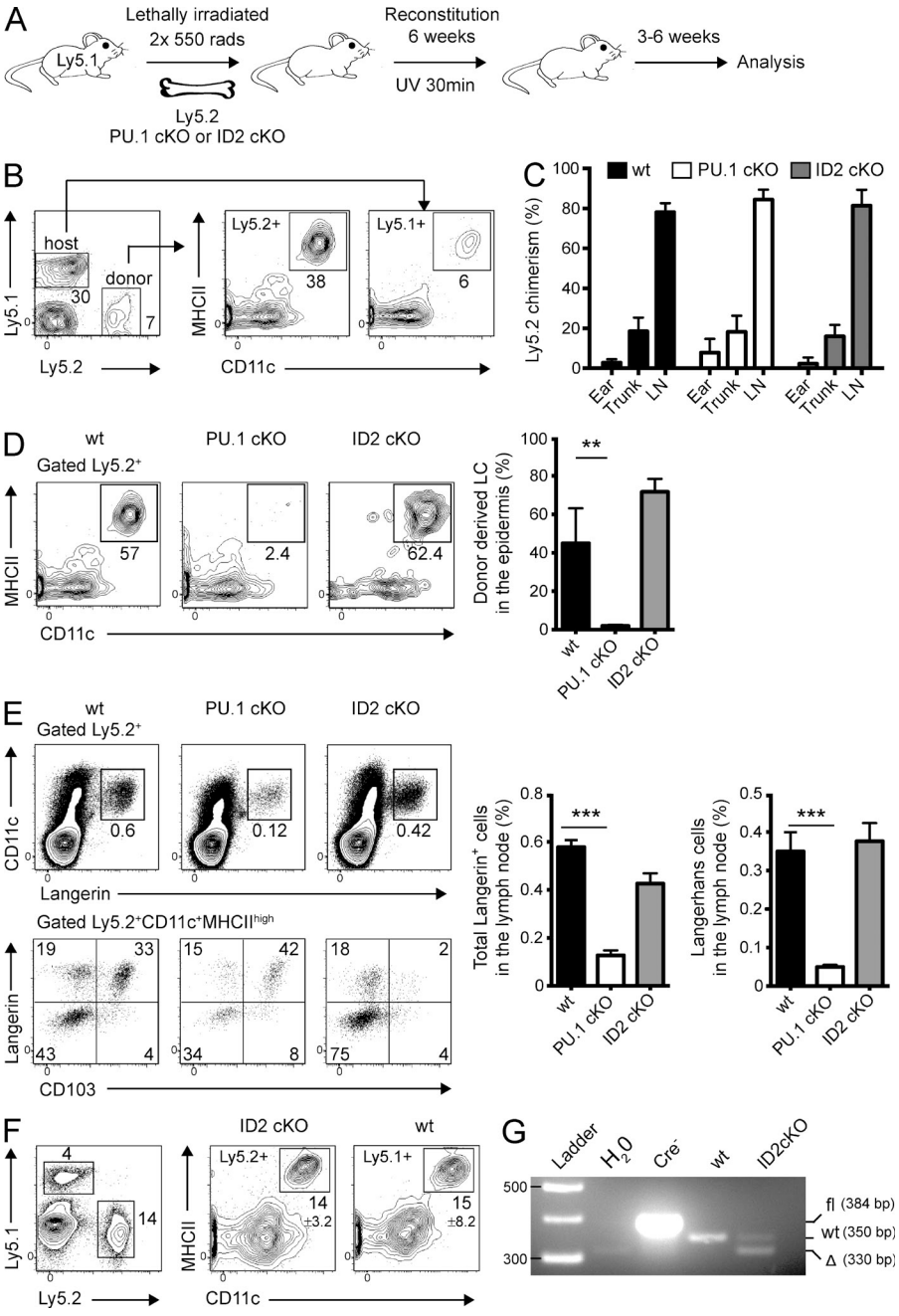

Figure 5. LC replenishment after UV induced inflammation depends on PU.1 but not ID2. (A) Schematic representation of the experimental plan. (B–E) Mice reconstituted with BM of the indicated genotype were exposed to UV and the repopulation of the epidermis by Ly5.2+ inflammatory LCs was assessed by flow cytometry after 3 wk. (B) Contour plot shows the expression of CD11c and MHCII in ear epidermal cells derived from wild-type (wt) donor (Ly5.2+) and host (Ly5.1+). Numbers represent the frequency of the gated populations. (C) Chart represents the mean frequency of chimerism ± SD for the indicated genotype in the ear, trunk, and LNs (n = 4/genotype). (D) Contour plot shows the expression of CD11c and MHCII in epidermal cells derived from donors of the indicated genotypes. Graphs show the mean frequency ± SD of donor-derived LCs found in the host epidermis from four mice per genotype. (E) Top left, expression of CD11c and Langerin in donor (Ly5.2+) cells of the indicated genotype from peripheral LNs. Bottom left, dot plots show the expression of CD103 and Langerin within Ly5.2+CD11c+MHCIIhigh cells. Numbers represent the frequency of the gated populations. Right, bar graphs show the mean proportion ± SD of either CD11c+Langerin+ LN cells (gated as in top left) or CD11c+Langerin+CD103− LCs (gated as in bottom left) derived from the indicated genotype. Data in B–E are representative of two independent experiments with at least four independent chimeric mice per genotype. **, $P < 0.01$; ***, $P < 0.001$ (unpaired Student's t test) compared with the wild-type sample. (F and G) Ly5.1 mice were reconstituted with BM from Id2cKO and exposed to UV. The repopulation of the epidermis by Ly5.2+ inflammatory LCs was assessed by flow cytometry after 6 wk. Contour plots show the expression of CD11c and MHCII in cells derived from donor (Ly5.2+, Id2cKO) and host (wt, ly5.1+) in the trunk. Numbers represent the mean frequency of LC ($n = 3 \pm$ SD) for the indicated compartment. (G) DNA was extracted from wild-type (Ly5.1+) and Id2cKO (Ly5.2+) BM-derived LC, gated as in F. The ID2 deletion efficiency was assessed by PCR. ID2cKO, CD11cCre−, *Id2*$^{fl/fl}$ and a wild-type control are shown. H_2O, no DNA added to the reaction. The position of the wild-type, loxP flanked (fl), and deleted (Δ) alleles are indicated. Numbers on the left indicate the molecular weight in base pairs. Data are representative of two independent experiments.

LCs, ID2 deletion did not affect LC differentiation in this setting, whereas PU.1 was found essential (Fig. 5, D–G).

Recently, it has been reported that during inflammation two distinct types of LCs seed the epidermis: a short-term LC, which persisted for up to 4 wk and was ID2 independent, and a long-term ID2-dependent LC (Seré et al., 2012). In that study, the short-term LC subset exhibited a distinct phenotype characterized by the lack of Langerin expression. In contrast the ID2cKO LCs that were present in the epidermis 3 wk after UV treatment in our experiments expressed Langerin in a manner indistinguishable from wild-type LCs (Fig. 6 B). As we have shown that all CD11c+MHCII+ cells expressed high PU.1^{GFP} (Fig. 6 A) and that MHCII and Langerin expression were exactly coincident (Fig. 6 B), we conclude that in our model all epidermal LCs were CD11c+MHCII+Langerin+ and PU.1^{GFP+}. Conversely the CD11c+MHCII−Langerin− cells lacked PU.1^{GFP} (Fig. 6) and instead expressed TCR-β or -γδ (Fig. 6 C).

These observations highlight that the LC network relies on two distinct transcriptional pathways, both of which are

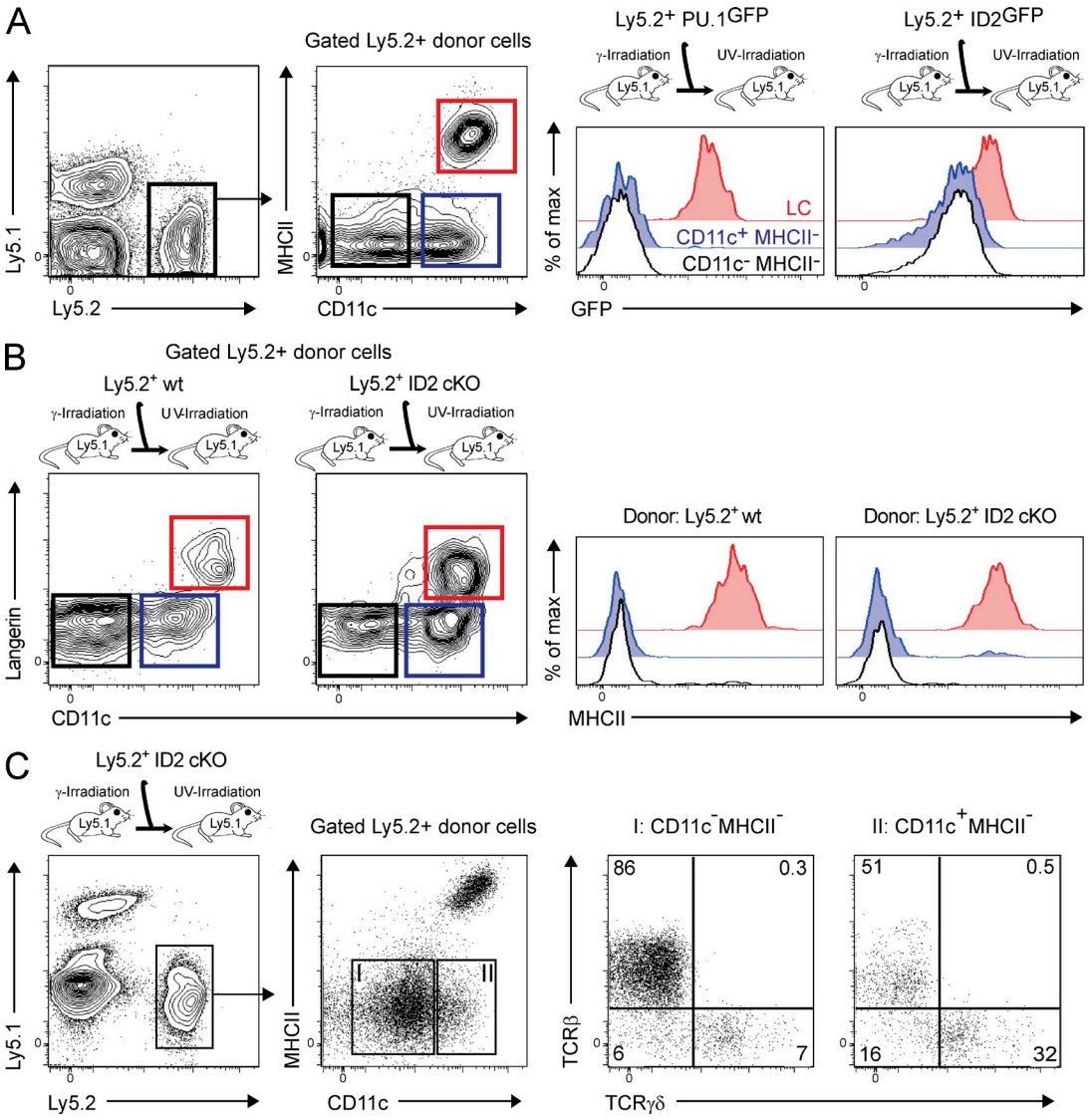

Figure 6. Inflammatory LCs express PU.1, ID2, and Langerin. (A and B) Donor cells (Ly5.2+) from either PU.1^{GFP} and ID2^{GFP} (A) or wild-type (wt) and ID2cKO mice (B) were subjected to the same experimental regimen outlined in Fig. 5 A. (A) Expression of GFP within the CD11c^{-}MHCII^{-} (black line), CD11c^{+}MHCII^{-} (filled blue), and CD11c^{+}MHCII^{+} inflammatory LC (filled red) fractions was determined by flow cytometry. (B) BM-derived LCs from wild-type or ID2cKO donors (Ly5.2+) were analyzed for expression of CD11c, Langerin, and MHCII by flow cytometry. Expression of MHCII within the CD11c^{-}Langerin^{-} (black line), CD11c^{+}Langerin^{-} (filled blue), and CD11c^{+}Langerin^{+} (filled red) fractions was determined by flow cytometry. (C) Leukocytes from ID2cKO donors (Ly5.2+) were analyzed for expression of CD11c and MHCII by flow cytometry. Gated Ly5.2^{+}CD11c^{-}MHCII^{-} (gate I) and Ly5.2^{+}CD11c^{+}MHCII^{-} (gate II) were examined for TCR-β and TCR-γδ by flow cytometry. Data in this figure are representative of two independent experiments.

PU.1 dependent. In addition, these results demonstrate that in vitro BM-derived LCs can be used as a surrogate system to study the molecular mechanisms involved in inflammation-induced LC differentiation in vivo, as LC differentiation in both models is PU.1 sensitive and ID2 insensitive.

PU.1 regulates RUNX3 expression in LCs

To further determine how PU.1 affects the differentiation of BM-derived LCs, we focused our analysis on the transcription factor RUNX3, which is pivotal in mediating LC differentiation in response to TGF-β (Fainaru et al., 2004). Real-time RT-PCR analysis showed that *Runx3* expression was strongly reduced in PU.1-deficient DC generated in vitro (Fig. 7 A). To determine whether PU.1 was able to directly regulate *Runx3* expression, BM cells from PU.1cKO were cultured in the presence of GM-CSF and TGF-β, and transduced with retroviral vectors expressing either GFP alone or with PU.1. Strikingly, RUNX3 expression was significantly increased in CD11c^{+}MHCII^{+} DCs ectopically expressing PU.1 compared with DCs expressing GFP alone (Fig. 7 B). LC numbers were increased in vitro when PU.1cKO cells were transduced with PU.1, suggesting that PU.1 controls *Runx3* expression in LCs (Fig. 7 C).

To examine whether PU.1 could regulate *Runx3* expression by direct binding to its regulatory elements, PU.1-bound

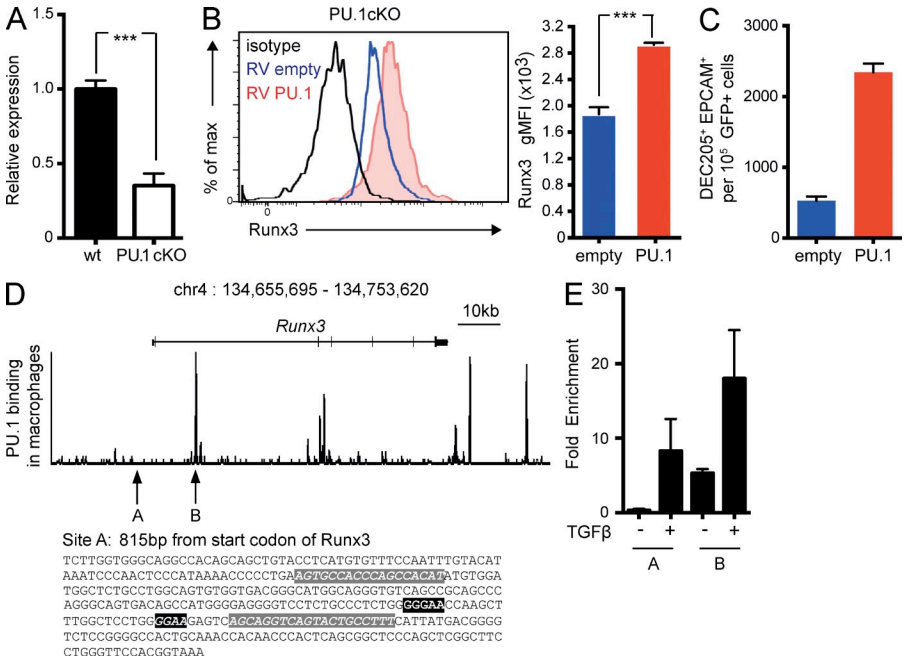

Figure 7. PU.1 regulates RUNX3 expression. (A) BM cells from wild-type (wt) and PU.1cKO mice were cultured for 3 d in the presence of GM-CSF and TGF-β. CD11c⁺MHCII⁺ cells were sorted and levels of *Runx3* were measured by quantitative real-time PCR. Graphs indicate the mean *Runx3* expression ± SD relative to *Hprt*. ***, $P < 0.001$ (unpaired Student's *t* test) for the indicated comparison. Data are representative of three independent experiments. (B) BM cells from PU.1cKO were transduced with either the empty vector (blue), or PU.1 (red)-expressing retroviruses (RV). RUNX3 expression in CD11c⁺MHCII⁺ DCs was measured by flow cytometry and compared with the isotype control (black line). Graph shows the geometric MFI ± SD of RUNX3 in transduced DCs with the indicated vector. ***, $P < 0.001$ (unpaired Student's *t* test) for the indicated comparison. (C) Mean numbers of CD11c⁺MHCII⁺DEC205⁺ EPCAM⁺ LCs ± SD generated after transduction of PU.1cKO BM with either empty vector (blue) or PU.1 (red). Data in B and C are representative of three independent experiments. (D) PU.1 binding at the *Runx3* locus as defined by ChIPseq analysis of BM derived macrophages. The PU.1 ChIPseq data have been previously described (Ghisletti et al., 2010). The PU.1 peaks that were subjected to further analysis in LCs are labeled A and B. Sequence below highlights additional putative PU.1 binding site (black boxes) found in the promoter of *Runx3*. Primers used for ChIP PCR are highlighted in gray. (E) Wild-type BM cells were cultured in GM-CSF ± TGF-β for 3 d. Binding of PU.1 to the regions labeled as A and B in D was analyzed by ChIP and enrichment was calculated by quantitative real time PCR as the mean fold of enrichment ± SD (compared with IgG control). Results are representative of two independent experiments.

DNA regions in myeloid cells were retrieved from the online available database (Ghisletti et al., 2010). PU.1 bound to several intronic and 3′ regions of the *Runx3* gene, most of which contained the PU.1 consensus core motif (GGAA, Fig. 7 D). In addition, in silico analysis of *Runx3* promoter showed other potential PU.1 binding sites. To test whether PU.1 directly binds in the *Runx3* gene in LCs, PU.1-bound chromatin was immunoprecipitated from wild-type cells cultured in the presence of GM-CSF ± TGF-β. Consistent with the ChIPseq data from macrophages, PU.1 was constitutively bound to the first intron of *Runx3*. Interestingly, although no binding of PU.1 to the *Runx3* promoter was observed in BM cells cultured in GM-CSF alone, the addition of TGF-β to the media induced the recruitment of PU.1 to *Runx3* promoter and also increased its binding to the intronic region (Fig. 7 E). Collectively, these observations suggest that PU.1 directly regulates *Runx3* expression in a TGF-β–dependent manner and thereby promotes LC differentiation.

RUNX3 expression rescues LC differentiation in the absence of PU.1

To test if the requirement of PU.1 for LC generation could be circumvented by constitutive expression of RUNX3, PU.1cKO BM cells were cultured in GM-CSF ± TGF-β and transduced with retroviral vectors expressing either GFP alone or with RUNX3. Strikingly, restoring RUNX3 expression could bypass the requirement of PU.1 to drive LC differentiation. Retroviral transduction of RUNX3 into wild-type BM precursors also increased the numbers of LCs generated by twofold when compared with control cultures, suggesting that the expression of RUNX3 is normally limiting for LC differentiation in vitro (Fig. 8 A).

A cardinal feature of the RUNX proteins is their highly conserved Runt domain, which is essential for DNA binding and protein–protein interaction (Ito, 2004). Alignment of the sequence coding for the Runt domains of RUNX1 and RUNX3 showed very high homology. The critical residues for RUNX1 DNA binding (arrows) were almost exclusively retained in the predicted DNA binding domain (box, Fig. 8 B), and were highly conserved in RUNX3 (Michaud et al., 2002; Li et al., 2003). Therefore, based on these similarities, a single point mutation within the last DNA contacting residue of RUNX3 ($RUNX3^{R196Q}$) was introduced and enabled to address the functionality of such mutant in promoting LC differentiation. Constitutive expression of $RUNX3^{R196Q}$ failed to promote enhanced LC differentiation in wild-type cells or to rescue the deficiency of PU.1cKO to differentiate into LCs (Fig. 8 C). Collectively, these results highlight the critical role for RUNX3 DNA binding in promoting LC differentiation and support the hypothesis that RUNX3 levels are a limiting factor for LC differentiation.

DISCUSSION

This study uses newly generated genetic tools to address the requirement of four transcription factors—PU.1, ID2, IRF4, and IRF8—in the development and/or maintenance of LCs.

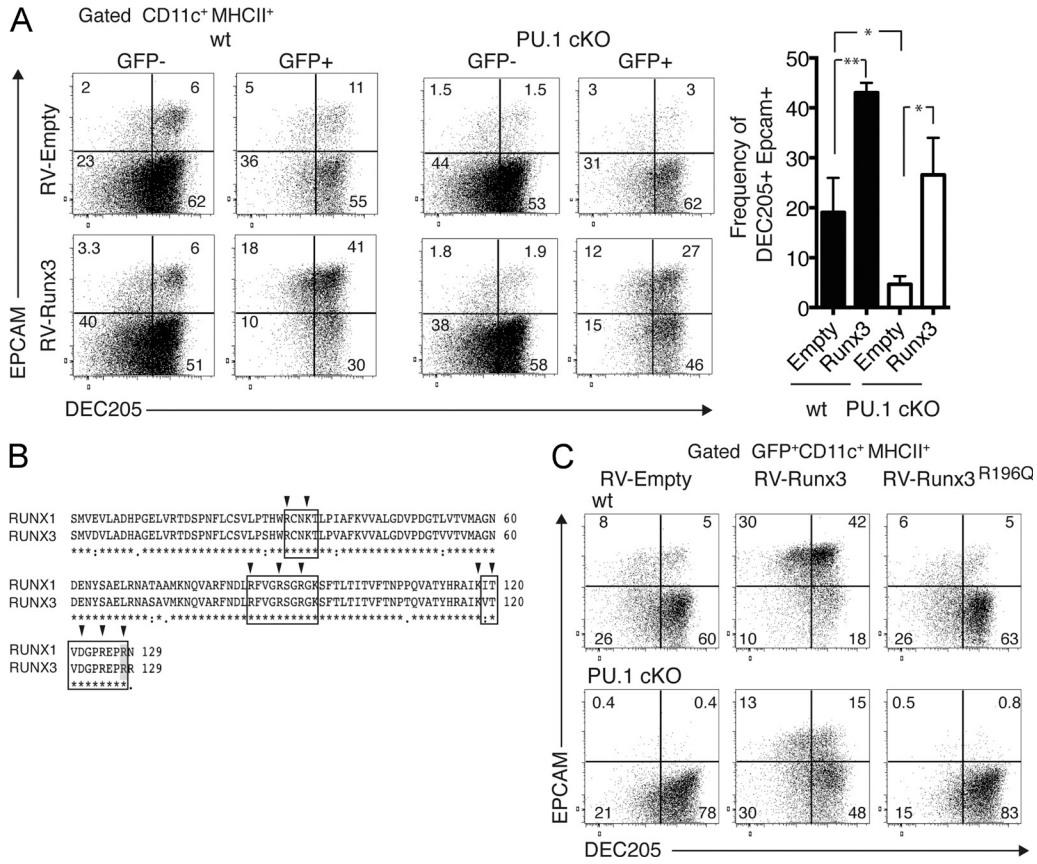

Figure 8. RUNX3 overexpression rescues LC differentiation in PU.1cKO. (A) BM cells of the indicated genotypes were transduced with either empty vector (RV-Empty) or a RUNX3 encoding retrovirus (RV-Runx3). Dot plot represents the expression of DEC205 and EPCAM in transduced (GFP+) or nontransduced (GFP−) CD11c+MHCII+ DCs 48 h after infection. Numbers indicate the percentage of cells in each quadrant. Graph shows the mean proportion ± SD of LCs generated with empty vector or Runx3 retrovirus. Data are representative of six independent experiments. *, $P < 0.05$; **, $P < 0.01$ (unpaired Student's *t* test) for the indicated comparisons. (B) Alignment (produced in clustalW) of the Runt domain from RUNX1 and RUNX3. Predicted DNA binding motifs are boxed (from Prosite). Arrowheads indicate the critical residues for RUNX1 DNA binding (as in Li et al., 2003). Gray shadowed residues indicate the position of the single mutation directed in RUNX3 construct. (C) The R196Q mutant of RUNX3 was generated by site directed mutation, and its functionality to promote LC differentiation was assessed by flow cytometry as in A. This experiment is representative of three independent experiments. Numbers indicate the percentage of cells in each quadrant.

Combining the use of reporter mice strains and the genetic ablation of these key transcription factors in a DC-specific manner, our study offers for the first time a comprehensive picture of the transcriptional network underlying LC homeostasis.

The detailed analysis of the expression pattern of PU.1, ID2, and IRF8 revealed their expression in the skin, whereas IRF4 was only up-regulated upon migration. LC numbers found in the LNs were considerably reduced in absence of IRF4, a finding which could be explained defects in either survival and/or migration in the absence of IRF4. Although EPCAM, an important regulator of LC migration (Gaiser et al., 2012), was normally expressed in the absence of IRF4 (unpublished data), IRF4 has also been shown to have a prominent role in promoting the expression of CCR7 in CD11b+ dermal DCs (Bajaña et al., 2012). CCR7 governs the migration of skin DCs under steady and inflammatory conditions. Yet CCR7 is not expressed on epidermal LCs. Therefore, one could speculate that upon maturation IRF4 up-regulation renders LCs sensitive and responsive to CCR7 ligands. The signaling events leading to IFR4 expression remain to be fully explored, but it will be important to address this question, as in some viral infections, such as HIV, infected LCs vehicle the viruses to the periphery and infect other DCs and T cells (Cunningham et al., 2008).

Epidermal LCs expressed a relatively low amount of IRF8, which was also up-regulated upon migration to the LN. However, IRF8 was found to be dispensable for LC homeostasis in the two mouse models (*Irf8*$^{-/-}$ and IRF8cKO) used in this study. This is in contrast to earlier observation made in *Irf8*$^{-/-}$ mice, where epidermal LC numbers and subsequent motility to the LNs were reduced (Schiavoni et al., 2004). Our results mirror recent observations that humans with dysfunctional IRF8—due to mutations that cripple its DNA binding activity—have a normal LC network, despite the severe immunodeficiency caused by the lack of circulating monocytes and DCs (Hambleton et al., 2011). Despite the

strong up-regulation of IRF8 expression in LN LCs, migration to the LN was also unaffected in IRF8cKO. Future studies should now address whether LCs are fully functional in the absence of IRF8.

In contrast to IRF4 and IRF8, steady-state LC development absolutely required ID2 and PU.1. In a screen designed to establish the transcriptional signature of DC development, ID2 was previously found to be a critical mediator of TGF-β signaling (Hacker et al., 2003). Consistent with this, both ID2- and TGF-β–deficient mice lack LCs (Borkowski et al., 1996; Strobl and Knapp, 1999; Hacker et al., 2003). To address the molecular function of ID2 and PU.1 in LC differentiation, we made use of an in vitro culture system, where addition of TGF-β has been shown to bias the differentiation of DC precursor into LC-like cells (Borkowski et al., 1996; Strobl and Knapp, 1999; Becker et al., 2011). These experiments showed that although the in vitro generation of BM-derived LCs was completely dependent on PU.1, the same process was insensitive to the loss of ID2, suggesting that the function of ID2 in LCs was context specific.

It has been shown that monocytes can be recruited to the inflamed skin and differentiate into LCs in response to external stress (Merad et al., 2002; Ginhoux et al., 2006; Nagao et al., 2012; Seré et al., 2012). One possible explanation for the differential requirement of steady-state epidermal LCs and in vitro–derived LCs for ID2 would be that the two populations were in fact generated from a distinct precursor, which relies on a distinct transcriptional network. To test this hypothesis, we made use of a model of inflammatory LC differentiation where circulating monocytes can be recruited to the dermis after UV-induced skin injury and differentiate into LCs (Merad et al., 2002; Ginhoux et al., 2006). Importantly, the results obtained in this in vivo setting mirrored the observation made in vitro as we observed that although donor-derived LCs expressed ID2, their development was ID2 independent.

Overall, the conclusion that inflammatory LCs do not depend on ID2 agrees with a recent study using ID2-null mice (Seré et al., 2012). However, those authors found that inflammatory LCs (termed short-term LCs in that study) did not express Langerin and thus were readily distinguishable from steady-state counterpart (Seré et al., 2012), whereas our data show that the LCs that repopulate the skin after inflammation expressed MHCII and Langerin to similar levels as steady-state LCs (Fig. 6). Similar to Sere et al. (2012), we also observed $CD11c^{+}Langerin^{-}$ cells; however, these cells lacked $PU.1^{GFP}$ expression and expressed the markers indicative of tissue-resident T cells. Sere et al. (2012) proposed that short-term LCs were ID2-independent and persisted for up to 4 wk after skin injury, after which they were replaced by $Langerin^{+}$, ID2-dependent cells they termed long-term LCs. In contrast, we found that the repopulation of injured epidermis with BM-derived LCs was in general ID2-independent and persisted for at least 6 wk. Some of these differences in the phenotype and longevity of the LCs may result from differences in the experimental setup, as Sere et al. (2012) used either $Id2^{-/-}$-null mice or alymphoid NOD/SCID/common γ chain$^{-/-}$ recipients in their transfer assays (Seré et al., 2012), both of which have severely compromised immune systems, whereas we used immune-competent wild-type (Ly5.1) mice which may react differently to the UV treatment. Despite these important differences, both studies support the conclusion that steady-state and inflammatory BM-derived LCs derive from distinct pathways that differ in their requirement for ID2.

We recently addressed the function of PU.1 in cDC and pDC differentiation and reported that PU.1 is essential to support the expression of *Flt3* in a dose-dependent manner (Carotta et al., 2010). A potential role for PU.1 in LC differentiation has been postulated; however, the underlying molecular mechanism was hitherto largely unexplored (Iwama et al., 2002; Heinz et al., 2006). The requirement for PU.1 in LCs is also not explained by the regulation of *Flt3* by PU.1 as Flt3 signaling is dispensable for LC homeostasis (Onai et al., 2007a; Merad et al., 2008; Waskow et al., 2008). One candidate target of PU.1 was the transcription factor RUNX3, which is pivotal to induce the signaling cascade mediated by TGF-β and thus LC formation (Fainaru et al., 2004). We found that PU.1 bound to *Runx3* regulatory elements, and its overexpression led to increased level of RUNX3, which ultimately promoted LC differentiation. RUNX3 appears to be a critical target of PU.1, as ectopic expression of RUNX3 alone was sufficient to restore LC formation in the absence of PU.1. In addition, RUNX3 overexpression in wild-type progenitors increased the number of precursors committing to the LC lineage. These results suggest that levels of RUNX3 are normally limiting for the differentiation of progenitors into mature LCs.

Interestingly, the PU.1 binding to the *Runx3* promoter was entirely dependent on TGF-β signaling, while the binding to an intronic sequence was enhanced by TGF-β. Thus, LC differentiation requires synergy between a major transcription factor (PU.1) and an extrinsic signal (TGF-β) to promote the expression of RUNX3, the lineage-defining transcription factor. The synergy between PU.1 and the TGF-β signaling pathway explains why ectopic PU.1 expression cannot promote LC generation in the absence of TGF-β (Heinz et al., 2006). Interestingly, several master regulatory transcription factors, including PU.1, have been shown to direct SMAD proteins to TGF-β targeted genes, thereby determining cell type–specific effect of TGF-β (Mullen et al., 2011). Therefore, it is tempting to speculate that the recruitment of PU.1 in a TGF-β–dependent manner at the promoter of *Runx3* poises the locus allowing the recruitment and co-occupancy of SMAD proteins, which ultimately drive *Runx3* transcription and LC differentiation.

In summary, our results provide important insights into the transcriptional circuitry driving LC homeostasis. We show that steady-state and inflammatory LCs rely on distinct transcriptional networks that are PU.1 regulated but differentially dependent on ID2. As the transcriptional network guiding their differentiation is different, this study also raises questions of whether or not steady-state and inflammatory LCs fulfill

distinct cutaneous immune functions. Our recently developed genetic tools gives us an unprecedented opportunity to explore this question in the future.

MATERIALS AND METHODS

Mice. *Sfpi1*$^{fl/fl}$ (Dakic et al., 2005), *Irf4*$^{fl/fl}$ (Klein et al., 2006), *Irf8*$^{fl/fl}$ (Feng et al., 2011), and *Id2*$^{fl/fl}$ (Seillet et al., 2013) mice were bred to the *Itgax*^{Cre} (Caton et al., 2007) strain that expresses Cre recombinase from the CD11c promoter. PCR assay for gene deletion was performed as described for *Sfpi1*$^{fl/fl}$ (Dakic et al., 2005) and *Id2*$^{fl/fl}$ (Seillet et al., 2013). Analysis of Cre-mediated deletion of the *Irf8*$^{fl/fl}$ allele was performed using primers A (5′-TTGGGGATTTC-CAGGCTGTTCTA-3′), B (5′-CACAGGGAGTCCCTCTTACAAT-3′), and C (5′-AACCACCAAGGCTGCAGCTGTTCAC-3′) to generate fragments of 214 bp (A/B wild type), ∼300 bp (A/B fl), and ∼700 bp (A/C exon2-deleted).

The PU.1^{GFP} (Nutt et al., 2005), ID2^{GFP} (Jackson et al., 2011), CX3CR1^{GFP} (Jung et al., 2000), *Irf4*$^{-/-}$ (Mittrücker et al., 1997), and *Irf8*$^{-/-}$ (Holtschke et al., 1996) strains have been previously described. *Itgax*^{Cre} and CX3CR1^{GFP} mice were obtained from The Jackson Laboratory. C57BL/6.Ly5.1 mice were maintained in house. Experiments involved 8–12-wk-old mice unless otherwise stated. Animal procedures were approved by The Walter and Eliza Hall Institute the Animal Ethics Committee.

Antibodies and flow cytometry. Antibodies against CD11c (N418), CD45.2 (A20), CD45.1 (104), MHCII (M514.15.2), CD8α (53–6.7), TCR-β (H57-597), TCR-γδ (GL3), and CD4 (GK1.4) were purchased from BD. Other antibodies were purchased from eBioscience (Ly6C [HK1.4] and CD103 [2E7]), Dendritics (Langerin [918A11]), BioLegend (EPCAM [13G8]), Santa Cruz Biotechnology, Inc. (IRF4), R&D Systems (RUNX3), or generated in house (DEC205 [NLDC205]).

Cells were resuspended in FACS buffer (PBS plus 0.5% BSA; Sigma-Aldrich), blocked with Fc block (eBioscience), and stained in FACS buffer at 4°C. For intracellular analysis, cells were fixed and permeabilized using Cytofix/Cytoperm kit (BD) according to the manufacturer's protocol. All analyses were performed on a FACS canto (BD) and data were analyzed using FlowJo software. Sorting was performed on a FACSAria (BD).

Cell isolation. Spleen and LNs were harvested, minced into fine pieces, and incubated for 30 min in FACS buffer containing collagenase and DNase (Gibco). For epidermal LC isolation, skin pieces (1 cm^2) were incubated for 1 h at 37°C in 2 U/ml Dispase (Gibco). After this treatment, epidermal sheets were peeled from the dermis, cut into fine pieces, and digested with 50 U/ml collagenase for 45 min at 37°C.

Immunofluorescence and confocal microscopy. Epidermal sheets were peeled from the dermis 30 min after treatment with 4% ammonium thiocyanate. Sheets were fixed in acetone for 5 min, blocked for 30 min with Fc block, and stained with anti-Langerin and anti-CD3 (2C11; produced in house). After five washes in PBS, slides were mounted in Fluoromount G medium (SouthernBiotech), imaged by confocal microscopy (LSM 780; Carl Zeiss), and then processed in ImageJ (vl.36b; National Institutes of Health).

Cell culture. Isolated BM cells were cultured in mouse tonicity RPMI-1640 supplemented with 10% heat inactivated fetal calf serum, 2 mM L-Glutamine (Gibco), 50 µM 2-mercaptoethanol (Sigma-Aldrich), and 100 U/ml penicillin/streptomycin (Gibco). 5×10^5 cells/ml were stimulated with 20 ng/ml GM-CSF (made in house) and 5 ng/ml TGF-β (or otherwise as indicated; eBioscience) for 3 d. For division tracking, BM cells were labeled with CFSE (Molecular Probes).

Retroviral transduction. The retroviral supernatants were produced using the pMIG-iresGFP (empty vector), pMIG-PU.1iresGFP, pMIG-RUNX-3iresGFP, and pMIG-RUNX3^{R196Q}iresGFP vectors as described in Carotta et al. (2010). 48 h after infection, cells were harvested and stained for flow cytometry analysis.

Skin inflammation. C57BL/6Ly5.1 mice were lethally irradiated (2 × 0.55 Gy), and reconstituted with Ly5.2$^+$ wild-type, *Itgax*^{cre}*Sfpi1*$^{fl/fl}$, or *Itgax*^{cre}*Id2*$^{fl/fl}$ BM. 6 wk after reconstitution, Ly5.1$^+$ LCs were depleted from the skin by exposing mice to UV for 30 min (wavelength 254 nm, voltage 8W, source: 38 cm). Replenishment of the LC network was assessed 3 or 6 wk after UV exposure.

RT-PCR. RNAs were isolated using RNeasy Plus Mini kit according to manufacturer's recommendations. cDNAs were synthesized from total RNAs with an oligo(dT) primers (Invitrogen) using Superscript III Reverse transcription according to the manufacturer's instructions. Amplification was performed with SYBR green master mix (Biolabs) on a CFX 384 (Bio-Rad Laboratories) using the primers described in Table S1.

Chromatin immunoprecipitation. 10^7 cells were cross-linked 1% paraformaldehyde (Sigma-Aldrich) in PBS and then lysed (1% SDS + 1 mM EDTA + protease inhibitors). Cross-linked DNA was sonicated with the Bioruptor (Diagenode). Protein G Dynabeads (Invitrogen) were incubated with 20 µg PU.1 antibody (T-20; Santa Cruz Biotechnology, Inc.) according to the manufacturer's protocol. Coupled antibody was added to 100 µg chromatin and incubated overnight at 4°C. Unbound chromatin was removed using a series of four washes. Following elution, bound chromatin was reverse cross-linked and subjected phenol/chloroform immunoprecipitation. Recovered DNA was resuspended in TE buffer and enrichment for specific region of the genome was measured by real-time PCR using the primers described in Table S2.

Online supplemental material. Fig. S1 shows in vitro generation of LCs, related to Fig. 2. Table S1 shows oligonucleotide primers for RT-PCR. Table S2 shows oligonucleotide primers for ChIP. Online supplemental material is available at http://www.jem.org/cgi/content/full/jem.20130930/DC1.

We thank U. Klein and T. Mak for mice, J. Leahy, N. Iannarella, R. Cole, M. Camilleri, and A. D'Amico and the institute flow cytometry facility for excellent technical assistance, and R. Allan and S. Naik for comments on the manuscript draft.

This work was supported by project grants (APP1048278 and APP1023266) and fellowships from the National Health and Medical Research Council (NHRMC) of Australia (to L. Wu, G.T. Belz, and S.L. Nutt), and the Intramural Research Program of the National Institutes of Health, National Institute of Allergy and Infectious Diseases (to H.C. Morse III). S.L. Nutt and G.T. Belz are supported by an Australian Research Council Future Fellowship. This work was made possible through Victorian State Government Operational Infrastructure Support and Australian Government NHMRC IRIIS.

The authors have no competing financial interests

Author contributions: M. Chopin designed, performed experiments and wrote the manuscript. S. Chevrier and C. Seillet analyzed data. H.C. Morse III, H. Wang, and L. Wu provided key reagents. S.L. Nutt and G.T. Belz supervised experimental design, analyzed data, and co-wrote the manuscript.

Submitted: 6 May 2013
Accepted: 24 October 2013

REFERENCES

Bachem, A., E. Hartung, S. Güttler, A. Mora, X. Zhou, A. Hegemann, M. Plantinga, E. Mazzini, P. Stoitzner, S. Gurka, et al. 2012. Expression of XCR1 characterizes the Batf3-dependent lineage of dendritic cells capable of antigen cross-presentation. *Front Immunol.* 3:214. http://dx.doi.org/10.3389/fimmu.2012.00214

Bajaña, S., K. Roach, S. Turner, J. Paul, and S. Kovats. 2012. IRF4 promotes cutaneous dendritic cell migration to lymph nodes during homeostasis and inflammation. *J. Immunol.* 189:3368–3377. http://dx.doi.org/10.4049/jimmunol.1102613

Becker, M.R., Y.S. Choi, S.E. Millar, and M.C. Udey. 2011. Wnt signaling influences the development of murine epidermal Langerhans cells. *J. Invest. Dermatol.* 131:1861–1868. http://dx.doi.org/10.1038/jid.2011.131

Belz, G.T., and S.L. Nutt. 2012. Transcriptional programming of the dendritic cell network. *Nat. Rev. Immunol.* 12:101–113. http://dx.doi.org/10.1038/nri3149

Borkowski, T.A., J.J. Letterio, A.G. Farr, and M.C. Udey. 1996. A role for endogenous transforming growth factor beta 1 in Langerhans cell biology: the skin of transforming growth factor beta 1 null mice is devoid of epidermal Langerhans cells. *J. Exp. Med.* 184:2417–2422. http://dx.doi.org/10.1084/jem.184.6.2417

Borkowski, T.A., J.J. Letterio, C.L. Mackall, A. Saitoh, X.J. Wang, D.R. Roop, R.E. Gress, and M.C. Udey. 1997. A role for TGFbeta1 in langerhans cell biology. Further characterization of the epidermal Langerhans cell defect in TGFbeta1 null mice. *J. Clin. Invest.* 100:575–581. http://dx.doi.org/10.1172/JCI119567

Bursch, L.S., L. Wang, B. Igyarto, A. Kissenpfennig, B. Malissen, D.H. Kaplan, and K.A. Hogquist. 2007. Identification of a novel population of Langerin$^+$ dendritic cells. *J. Exp. Med.* 204:3147–3156. http://dx.doi.org/10.1084/jem.20071966

Carotta, S., A. Dakic, A. D'Amico, S.H. Pang, K.T. Greig, S.L. Nutt, and L. Wu. 2010. The transcription factor PU.1 controls dendritic cell development and Flt3 cytokine receptor expression in a dose-dependent manner. *Immunity.* 32:628–641. http://dx.doi.org/10.1016/j.immuni.2010.05.005

Caton, M.L., M.R. Smith-Raska, and B. Reizis. 2007. Notch-RBP-J signaling controls the homeostasis of CD8$^-$ dendritic cells in the spleen. *J. Exp. Med.* 204:1653–1664.

Chorro, L., A. Sarde, M. Li, K.J. Woollard, P. Chambon, B. Malissen, A. Kissenpfennig, J.B. Barbaroux, R. Groves, and F. Geissmann. 2009. Langerhans cell (LC) proliferation mediates neonatal development, homeostasis, and inflammation-associated expansion of the epidermal LC network. *J. Exp. Med.* 206:3089–3100. http://dx.doi.org/10.1084/jem.20091586

Crozat, K., S. Tamoutounour, T.P. Vu Manh, E. Fossum, H. Luche, L. Ardouin, M. Guilliams, H. Azukizawa, B. Bogen, B. Malissen, et al. 2011. Cutting edge: expression of XCR1 defines mouse lymphoid-tissue resident and migratory dendritic cells of the CD8α+ type. *J. Immunol.* 187:4411–4415. http://dx.doi.org/10.4049/jimmunol.1101717

Cunningham, A.L., F. Carbone, and T.B. Geijtenbeek. 2008. Langerhans cells and viral immunity. *Eur. J. Immunol.* 38:2377–2385. http://dx.doi.org/10.1002/eji.200838521

Dakic, A., D. Metcalf, L. Di Rago, S. Mifsud, L. Wu, and S.L. Nutt. 2005. PU.1 regulates the commitment of adult hematopoietic progenitors and restricts granulopoiesis. *J. Exp. Med.* 201:1487–1502. http://dx.doi.org/10.1084/jem.20050075

Dakic, A., L. Wu, and S.L. Nutt. 2007. Is PU.1 a dosage-sensitive regulator of haemopoietic lineage commitment and leukaemogenesis? *Trends Immunol.* 28:108–114. http://dx.doi.org/10.1016/j.it.2007.01.006

Edelson, B.T., W. Kc, R. Juang, M. Kohyama, L.A. Benoit, P.A. Klekotka, C. Moon, J.C. Albring, W. Ise, D.G. Michael, et al. 2010. Peripheral CD103$^+$ dendritic cells form a unified subset developmentally related to CD8α$^+$ conventional dendritic cells. *J. Exp. Med.* 207:823–836. http://dx.doi.org/10.1084/jem.20091627

Edelson, B.T., T.R. Bradstreet, W. Kc, K. Hildner, J.W. Herzog, J. Sim, J.H. Russell, T.L. Murphy, E.R. Unanue, and K.M. Murphy. 2011. Batf3-dependent CD11b(low/-) peripheral dendritic cells are GM-CSF-independent and are not required for Th cell priming after subcutaneous immunization. *PLoS ONE.* 6:e25660. http://dx.doi.org/10.1371/journal.pone.0025660

Fainaru, O., E. Woolf, J. Lotem, M. Yarmus, O. Brenner, D. Goldenberg, V. Negreanu, Y. Bernstein, D. Levanon, S. Jung, and Y. Groner. 2004. Runx3 regulates mouse TGF-beta-mediated dendritic cell function and its absence results in airway inflammation. *EMBO J.* 23:969–979. http://dx.doi.org/10.1038/sj.emboj.7600085

Feng, J., H. Wang, D.M. Shin, M. Masiuk, C.F. Qi, and H.C. Morse III. 2011. IFN regulatory factor 8 restricts the size of the marginal zone and follicular B cell pools. *J. Immunol.* 186:1458–1466. http://dx.doi.org/10.4049/jimmunol.1001950

Gaiser, M.R., T. Lämmermann, X. Feng, B.Z. Igyarto, D.H. Kaplan, L. Tessarollo, R.N. Germain, and M.C. Udey. 2012. Cancer-associated epithelial cell adhesion molecule (EpCAM; CD326) enables epidermal Langerhans cell motility and migration in vivo. *Proc. Natl. Acad. Sci. USA.* 109:E889–E897. http://dx.doi.org/10.1073/pnas.1117674109

Geissmann, F., C. Prost, J.P. Monnet, M. Dy, N. Brousse, and O. Hermine. 1998. Transforming growth factor β1, in the presence of granulocyte/macrophage colony-stimulating factor and interleukin 4, induces differentiation of human peripheral blood monocytes into dendritic Langerhans cells. *J. Exp. Med.* 187:961–966. http://dx.doi.org/10.1084/jem.187.6.961

Geissmann, F., S. Jung, and D.R. Littman. 2003. Blood monocytes consist of two principal subsets with distinct migratory properties. *Immunity.* 19:71–82. http://dx.doi.org/10.1016/S1074-7613(03)00174-2

Ghisletti, S., I. Barozzi, F. Mietton, S. Polletti, F. De Santa, E. Venturini, L. Gregory, L. Lonie, A. Chew, C.L. Wei, et al. 2010. Identification and characterization of enhancers controlling the inflammatory gene expression program in macrophages. *Immunity.* 32:317–328. http://dx.doi.org/10.1016/j.immuni.2010.02.008

Ginhoux, F., F. Tacke, V. Angeli, M. Bogunovic, M. Loubeau, X.M. Dai, E.R. Stanley, G.J. Randolph, and M. Merad. 2006. Langerhans cells arise from monocytes in vivo. *Nat. Immunol.* 7:265–273. http://dx.doi.org/10.1038/ni1307

Ginhoux, F., K. Liu, J. Helft, M. Bogunovic, M. Greter, D. Hashimoto, J. Price, N. Yin, J. Bromberg, S.A. Lira, et al. 2009. The origin and development of nonlymphoid tissue CD103$^+$ DCs. *J. Exp. Med.* 206:3115–3130. http://dx.doi.org/10.1084/jem.20091756

Greter, M., I. Lelios, P. Pelczar, G. Hoeffel, J. Price, M. Leboeuf, T.M. Kündig, K. Frei, F. Ginhoux, M. Merad, and B. Becher. 2012. Stroma-derived interleukin-34 controls the development and maintenance of langerhans cells and the maintenance of microglia. *Immunity.* 37:1050–1060. http://dx.doi.org/10.1016/j.immuni.2012.11.001

Hacker, C., R.D. Kirsch, X.S. Ju, T. Hieronymus, T.C. Gust, C. Kuhl, T. Jorgas, S.M. Kurz, S. Rose-John, Y. Yokota, and M. Zenke. 2003. Transcriptional profiling identifies Id2 function in dendritic cell development. *Nat. Immunol.* 4:380–386. http://dx.doi.org/10.1038/ni903

Hambleton, S., S. Salem, J. Bustamante, V. Bigley, S. Boisson-Dupuis, J. Azevedo, A. Fortin, M. Haniffa, L. Ceron-Gutierrez, C.M. Bacon, et al. 2011. IRF8 mutations and human dendritic-cell immunodeficiency. *N. Engl. J. Med.* 365:127–138. http://dx.doi.org/10.1056/NEJMoa1100066

Hashimoto, D., J. Miller, and M. Merad. 2011. Dendritic cell and macrophage heterogeneity in vivo. *Immunity.* 35:323–335. http://dx.doi.org/10.1016/j.immuni.2011.09.007

Heinz, L.X., B. Platzer, P.M. Reisner, A. Jörgl, S. Taschner, F. Göbel, and H. Strobl. 2006. Differential involvement of PU.1 and Id2 downstream of TGF-beta1 during Langerhans-cell commitment. *Blood.* 107:1445–1453. http://dx.doi.org/10.1182/blood-2005-04-1721

Hildner, K., B.T. Edelson, W.E. Purtha, M. Diamond, H. Matsushita, M. Kohyama, B. Calderon, B.U. Schraml, E.R. Unanue, M.S. Diamond, et al. 2008. Batf3 deficiency reveals a critical role for CD8alpha+ dendritic cells in cytotoxic T cell immunity. *Science.* 322:1097–1100. http://dx.doi.org/10.1126/science.1164206

Hoeffel, G., Y. Wang, M. Greter, P. See, P. Teo, B. Malleret, M. Leboeuf, D. Low, G. Oller, F. Almeida, et al. 2012. Adult Langerhans cells derive predominantly from embryonic fetal liver monocytes with a minor contribution of yolk sac-derived macrophages. *J. Exp. Med.* 209:1167–1181. http://dx.doi.org/10.1084/jem.20120340

Holtschke, T., J. Löhler, Y. Kanno, T. Fehr, N. Giese, F. Rosenbauer, J. Lou, K.P. Knobeloch, L. Gabriele, J.F. Waring, et al. 1996. Immunodeficiency and chronic myelogenous leukemia-like syndrome in mice with a targeted mutation of the ICSBP gene. *Cell.* 87:307–317. http://dx.doi.org/10.1016/S0092-8674(00)81348-3

Ito, Y. 2004. Oncogenic potential of the RUNX gene family: 'overview'. *Oncogene.* 23:4198–4208. http://dx.doi.org/10.1038/sj.onc.1207755

Iwama, A., M. Osawa, R. Hirasawa, N. Uchiyama, S. Kaneko, M. Onodera, K. Shibuya, A. Shibuya, C. Vinson, D.G. Tenen, and H. Nakauchi. 2002. Reciprocal roles for CCAAT/enhancer binding protein (C/EBP) and PU.1 transcription factors in Langerhans cell commitment. *J. Exp. Med.* 195:547–558. http://dx.doi.org/10.1084/jem.20011465

Jackson, J.T., Y. Hu, R. Liu, F. Masson, A. D'Amico, S. Carotta, A. Xin, M.J. Camilleri, A.M. Mount, A. Kallies, et al. 2011. Id2 expression delineates differential checkpoints in the genetic program of CD8α+

and CD103+ dendritic cell lineages. *EMBO J.* 30:2690–2704. http://dx.doi.org/10.1038/emboj.2011.163

Jung, S., J. Aliberti, P. Graemmel, M.J. Sunshine, G.W. Kreutzberg, A. Sher, and D.R. Littman. 2000. Analysis of fractalkine receptor CX(3)CR1 function by targeted deletion and green fluorescent protein reporter gene insertion. *Mol. Cell. Biol.* 20:4106–4114. http://dx.doi.org/10.1128/MCB.20.11.4106-4114.2000

Klein, U., S. Casola, G. Cattoretti, Q. Shen, M. Lia, T. Mo, T. Ludwig, K. Rajewsky, and R. Dalla-Favera. 2006. Transcription factor IRF4 controls plasma cell differentiation and class-switch recombination. *Nat. Immunol.* 7:773–782. http://dx.doi.org/10.1038/ni1357

Li, Z., J. Yan, C.J. Matheny, T. Corpora, J. Bravo, A.J. Warren, J.H. Bushweller, and N.A. Speck. 2003. Energetic contribution of residues in the Runx1 Runt domain to DNA binding. *J. Biol. Chem.* 278:33088–33096. http://dx.doi.org/10.1074/jbc.M303973200

Liao, X., N. Sharma, F. Kapadia, G. Zhou, Y. Lu, H. Hong, K. Paruchuri, G.H. Mahabeleshwar, E. Dalmas, N. Venteclef, et al. 2011. Krüppel-like factor 4 regulates macrophage polarization. *J. Clin. Invest.* 121:2736–2749. http://dx.doi.org/ 10.1172/JCI45444

McKenna, H.J., K.L. Stocking, R.E. Miller, K. Brasel, T. De Smedt, E. Maraskovsky, C.R. Maliszewski, D.H. Lynch, J. Smith, B. Pulendran, et al. 2000. Mice lacking flt3 ligand have deficient hematopoiesis affecting hematopoietic progenitor cells, dendritic cells, and natural killer cells. *Blood.* 95:3489–3497.

Merad, M., M.G. Manz, H. Karsunky, A. Wagers, W. Peters, I. Charo, I.L. Weissman, J.G. Cyster, and E.G. Engleman. 2002. Langerhans cells renew in the skin throughout life under steady-state conditions. *Nat. Immunol.* 3:1135–1141. http://dx.doi.org/10.1038/ni852

Merad, M., F. Ginhoux, and M. Collin. 2008. Origin, homeostasis and function of Langerhans cells and other langerin-expressing dendritic cells. *Nat. Rev. Immunol.* 8:935–947. http://dx.doi.org/10.1038/nri2455

Michaud, J., F. Wu, M. Osato, G.M. Cottles, M. Yanagida, N. Asou, K. Shigesada, Y. Ito, K.F. Benson, W.H. Raskind, et al. 2002. In vitro analyses of known and novel RUNX1/AML1 mutations in dominant familial platelet disorder with predisposition to acute myelogenous leukemia: implications for mechanisms of pathogenesis. *Blood.* 99:1364–1372. http://dx.doi.org/10.1182/blood.V99.4.1364

Mittrücker, H.W., T. Matsuyama, A. Grossman, T.M. Kündig, J. Potter, A. Shahinian, A. Wakeham, B. Patterson, P.S. Ohashi, and T.W. Mak. 1997. Requirement for the transcription factor LSIRF/IRF4 for mature B and T lymphocyte function. *Science.* 275:540–543. http://dx.doi.org/10.1126/science.275.5299.540

Mullen, A.C., D.A. Orlando, J.J. Newman, J. Lovén, R.M. Kumar, S. Bilodeau, J. Reddy, M.G. Guenther, R.P. DeKoter, and R.A. Young. 2011. Master transcription factors determine cell-type-specific responses to TGF-β signaling. *Cell.* 147:565–576. http://dx.doi.org/10.1016/j.cell.2011.08.050

Nagao, K., T. Kobayashi, K. Moro, M. Ohyama, T. Adachi, D.Y. Kitashima, S. Ueha, K. Horiuchi, H. Tanizaki, K. Kabashima, et al. 2012. Stress-induced production of chemokines by hair follicles regulates the trafficking of dendritic cells in skin. *Nat. Immunol.* 13:744–752. http://dx.doi.org/10.1038/ni.2353

Naik, S.H., P. Sathe, H.Y. Park, D. Metcalf, A.I. Proietto, A. Dakic, S. Carotta, M. O'Keeffe, M. Bahlo, A. Papenfuss, et al. 2007. Development of plasmacytoid and conventional dendritic cell subtypes from single precursor cells derived in vitro and in vivo. *Nat. Immunol.* 8:1217–1226. http://dx.doi.org/10.1038/ni1522

Nutt, S.L., D. Metcalf, A. D'Amico, M. Polli, and L. Wu. 2005. Dynamic regulation of PU.1 expression in multipotent hematopoietic progenitors. *J. Exp. Med.* 201:221–231. http://dx.doi.org/10.1084/jem.20041535

Onai, N., A. Obata-Onai, M.A. Schmid, and M.G. Manz. 2007a. Flt3 in regulation of type I interferon-producing cell and dendritic cell development. *Ann. N.Y. Acad. Sci.* 1106:253–261. http://dx.doi.org/10.1196/annals.1392.015

Onai, N., A. Obata-Onai, M.A. Schmid, T. Ohteki, D. Jarrossay, and M.G. Manz. 2007b. Identification of clonogenic common Flt3+M-CSFR+ plasmacytoid and conventional dendritic cell progenitors in mouse bone marrow. *Nat. Immunol.* 8:1207–1216. http://dx.doi.org/10.1038/ni1518

Sathe, P., J. Pooley, D. Vremec, J. Mintern, J.O. Jin, L. Wu, J.Y. Kwak, J.A. Villadangos, and K. Shortman. 2011. The acquisition of antigen cross-presentation function by newly formed dendritic cells. *J. Immunol.* 186:5184–5192. http://dx.doi.org/10.4049/jimmunol.1002683

Schiavoni, G., F. Mattei, P. Borghi, P. Sestili, M. Venditti, H.C. Morse III, F. Belardelli, and L. Gabriele. 2004. ICSBP is critically involved in the normal development and trafficking of Langerhans cells and dermal dendritic cells. *Blood.* 103:2221–2228. http://dx.doi.org/10.1182/blood-2003-09-3007

Seillet, C., J.T. Jackson, K.A. Markey, H.J. Brady, G.R. Hill, K.P. Macdonald, S.L. Nutt, and G.T. Belz. 2013. CD8α+ DCs can be induced in the absence of transcription factors Id2, Nfil3, and Batf3. *Blood.* 121:1574–1583. http://dx.doi.org/10.1182/blood-2012-07-445650

Seré, K., J.H. Baek, J. Ober-Blöbaum, G. Müller-Newen, F. Tacke, Y. Yokota, M. Zenke, and T. Hieronymus. 2012. Two distinct types of Langerhans cells populate the skin during steady state and inflammation. *Immunity.* 37:905–916. http://dx.doi.org/10.1016/j.immuni.2012.07.019

Strobl, H., and W. Knapp. 1999. TGF-beta1 regulation of dendritic cells. *Microbes Infect.* 1:1283–1290. http://dx.doi.org/10.1016/S1286-4579(99)00256-7

Tripp, C.H., S. Chang-Rodriguez, P. Stoitzner, S. Holzmann, H. Stössel, P. Douillard, S. Saeland, F. Koch, A. Elbe-Bürger, and N. Romani. 2004. Ontogeny of Langerin/CD207 expression in the epidermis of mice. *J. Invest. Dermatol.* 122:670–672. http://dx.doi.org/10.1111/j.0022-202X.2004.22337.x

Tussiwand, R., N. Onai, L. Mazzucchelli, and M.G. Manz. 2005. Inhibition of natural type I IFN-producing and dendritic cell development by a small molecule receptor tyrosine kinase inhibitor with Flt3 affinity. *J. Immunol.* 175:3674–3680.

Wang, Y., K.J. Szretter, W. Vermi, S. Gilfillan, C. Rossini, M. Cella, A.D. Barrow, M.S. Diamond, and M. Colonna. 2012. IL-34 is a tissue-restricted ligand of CSF1R required for the development of Langerhans cells and microglia. *Nat. Immunol.* 13:753–760. http://dx.doi.org/10.1038/ni.2360

Waskow, C., K. Liu, G. Darrasse-Jèze, P. Guermonprez, F. Ginhoux, M. Merad, T. Shengelia, K. Yao, and M. Nussenzweig. 2008. The receptor tyrosine kinase Flt3 is required for dendritic cell development in peripheral lymphoid tissues. *Nat. Immunol.* 9:676–683. http://dx.doi.org/10.1038/ni.1615

Witmer-Pack, M.D., D.A. Hughes, G. Schuler, L. Lawson, A. McWilliam, K. Inaba, R.M. Steinman, and S. Gordon. 1993. Identification of macrophages and dendritic cells in the osteopetrotic (op/op) mouse. *J. Cell Sci.* 104:1021–1029.